Methods and results of acoustical measurements made of a Delta IV Heavy launch

Grant W. Hart, Logan T. Mathews, Mark C. Anderson, et al.

Citation: Proc. Mtgs. Acoust. **45**, 040003 (2021); doi: 10.1121/2.0001580
View online: https://doi.org/10.1121/2.0001580
View Table of Contents: https://asa.scitation.org/toc/pma/45/1
Published by the Acoustical Society of America

ARTICLES YOU MAY BE INTERESTED IN

Characterization of Falcon 9 launch vehicle noise from far-field measurements
The Journal of the Acoustical Society of America **150**, 620 (2021); https://doi.org/10.1121/10.0005658

Acoustical measurements of a Delta IV Heavy launch (NROL-82)
The Journal of the Acoustical Society of America **150**, A177 (2021); https://doi.org/10.1121/10.0008038

Supersonic jet noise from launch vehicles: 50 years since NASA SP-8072
The Journal of the Acoustical Society of America **151**, 752 (2022); https://doi.org/10.1121/10.0009160

High-fidelity sonic boom measurements using weather-robust measurement equipment
Proceedings of Meetings on Acoustics **39**, 040005 (2019); https://doi.org/10.1121/2.0001578

Comparing two weather-robust microphone configurations for outdoor measurements
Proceedings of Meetings on Acoustics **42**, 040005 (2020); https://doi.org/10.1121/2.0001561

Estimation of uncertainties in underwater sound measurements of ships
Proceedings of Meetings on Acoustics **47**, 070002 (2022); https://doi.org/10.1121/2.0001571

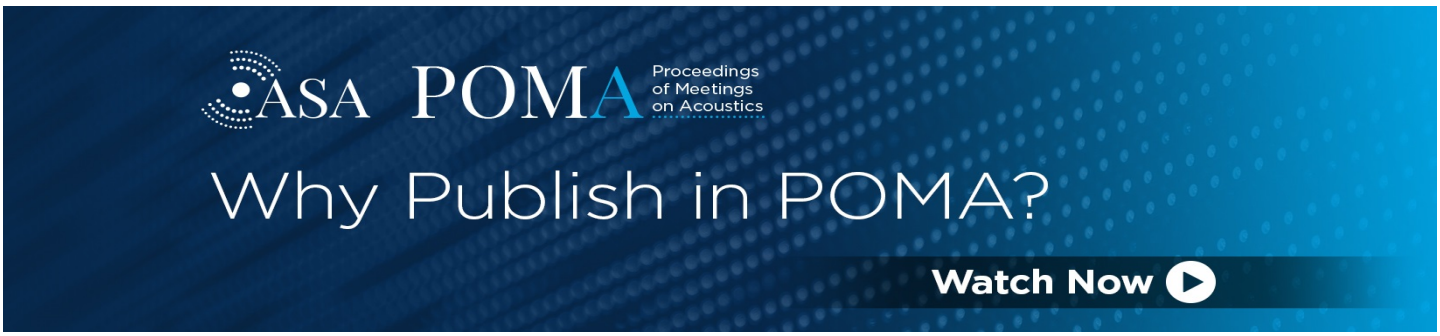

Proceedings of Meetings on Acoustics

Volume 45 http://acousticalsociety.org/

181st Meeting of the Acoustical Society of America

Seattle, Washington

29 November - 3 December 2021

Noise: Paper 3aNS6

Methods and results of acoustical measurements made of a Delta IV Heavy launch

Grant W. Hart, Logan T. Mathews, Mark C. Anderson, J. Taggart Durrant, Michael S. Bassett, Samuel A. Olausson, Griffin Houston and Kent L. Gee

Department of Physics and Astronomy, Brigham Young University, Provo, UT, 84602; grant_hart@byu.edu; loganmathews103@gmail.com; anderson.mark.az@gmail.com; taggart.durrant@gmail.com; michaelbassett3of8@gmail.com; samolausson@gmail.com; griffin.a.houston@gmail.com; kentgee@byu.edu

On April 26, 2021 the Brigham Young University (BYU) acoustics research group made a number of acoustic noise measurements during the launch of a Delta IV Heavy rocket from Vandenberg Space Force Base in California. The sensors ranged in distance from 330 m to 19 km from the launch site. Some sensors were arranged in a rough arc of 1-2 km radius and others were placed along both an east-west line and a north-south line. This enabled the measurement of the distribution of the noise in the different directions and at different distances. Two of the sensors were 5-meter radius, 4-microphone intensity probes. Using these probes it was possible to track the trajectory of the rocket ascent; the acoustically traced trajectory agrees well with the trajectory data obtained from Vandenberg. The measurements showed that the peak directivity of the launch vehicle noise was at 70.4±2.1 degrees relative to the plume direction. The total acoustic power level was found to be 197 dB re 1 pW. This represents an acoustic radiation efficiency of about 0.3%, somewhat lower than is normally assumed.

Published by the Acoustical Society of America

© 2022 Acoustical Society of America. https://doi.org/10.1121/2.0001580

1. INTRODUCTION

The world is undergoing a large increase in the number of rocket launches as a number of new companies and countries are attempting to launch satellites and other missions to space. In the year 2021 there were more orbital launch attempts and successful launches than in any previous year, with 2022 projected to have about a 50% increase in launch number over 2021.[1] This increase in launch frequency carries with it a need to better understand the noise produced, and effects on the surrounding communities and natural environment, by different launch vehicles.

The current knowledge of launch vehicle noise is based on measurements made by NASA in the 1950s and 1960s[2–7] and augmented by work done in the 1990s and 2000s by McInerny,[8–13] but much of that work is difficult to find and done using equipment and methods that, while state of the art at the time, are now superseded by more modern techniques. We also have a better theoretical understanding of the sources and causes of the noise produced by jets and rockets,[1] but much is still unstudied.

On April 26, 2021 a group of researchers from Brigham Young University (BYU) made measurements of the launch of the NROL-82 mission from Vandenberg Space Force Base on a Delta IV Heavy launch vehicle. This paper describes the measurement plan and describes the some preliminary results of those measurements.

A. THE DELTA IV HEAVY LAUNCH VEHICLE

The Delta IV Heavy launch vehicle consists of three Common Booster Core modules arranged in a straight line (see Fig 1.) Each module uses an RS-68A engine that is fueled by liquid hydrogen and liquid oxygen (LH2/LOX). This is currently the second-highest-capacity launch vehicle (by payload weight to low-Earth orbit) in current use, behind SpaceX's Falcon Heavy.

2. MEASUREMENT PLAN FOR NROL-82

Twelve stations were used to record the launch, three attended and nine autonomous. Figure 2 shows the positioning of the measurment stations relative to the launch site. Several were located in a rough arc at a distance of 1000-1500 m from the pad. Others were located near a north-south line and on an east-west line, ranging in distance from 1000 m to 19.6 km. One station was located close to the pad itself at a distance of 330 m. The exact locations were determined by accessibility via road on base.

A. EQUIPMENT

Each station consisted of a weatherproof box[14] that contained a Windows tablet-style computer, a data acquisition system consisting of National Instruments model 9171 or 9174 acquisition chassis with either 9250 or 9232 data acquisition modules. Each station also had a GPS receiver to allow for absolute timing of the data. On the outside of each box there were one to five GRAS 1/4" or 1/2" microphones, depending on the station, enclosed in windscreens with ground plates.[15] The 1/4" microphones have a frequency range of about 4 Hz - 70 kHz, and the 1/2" microphones were infrasound microphones with a frequency range of 0.09 Hz - 20 kHz. Each box was powered by an auxiliary battery, with most of them connected to a solar charging panel.

Figure 3 shows both a photograph of a typical station and the data taken at that station, along with the maximum 1-s Overall Sound Pressue Level (OASPL) of the data. Note the asymmetry of the amplitude waveform, with the positive pressure excursions being as much as 2 1/2 times as high as the negative excursions near the peak. Positive pressure skewness has been observed in prior rocket launch[9] and military aircraft data.[16] Also note the relatively high background noise level of 92-97 dB, caused by the windy day. A typical background OASPL for these locations on a calm day is around 65-70 dB.

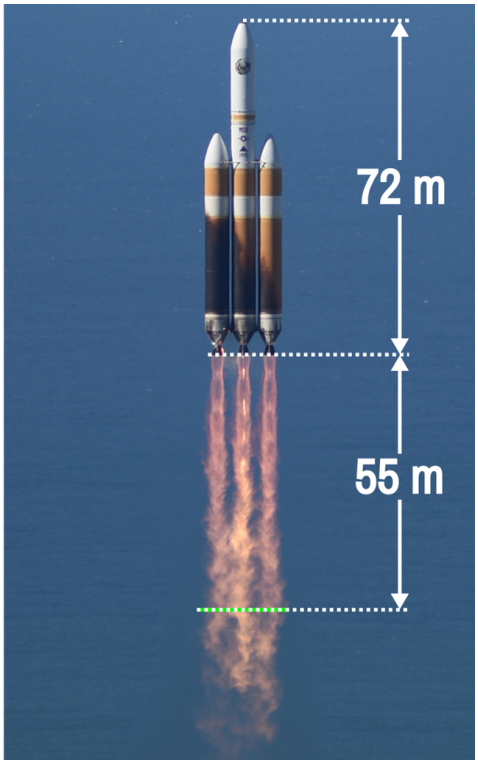

Figure 1: Picture of a Delta IV Heavy rocket shortly after liftoff. The rocket's height is 72 m and the apparent peak sound source was measured to be 55 m below the nozzles, as shown. Note that the plumes are not yet fully merged at this point. Photo credit: Michael Peterson/USAF

3. SPECTRAL CHARACTERISTICS

In Fig. 4 we see the one-third octave spectra of the launch along both the eastern radial and the northern radial during the time of peak OASPL. The spectra are computed between the 3 dB-down points on both sides of the peak OASPL at each station. At close stations the spectrum drops at about 10 dB/decade, characteristic of nonlinear shock propagation,[17] as can be seen by comparison to the dashed magenta line on the figure. In all cases the earlier roll-off of the higher frequencies from the 10 dB/decade line with distance is apparent as the shocks in the waveforms broaden. Characteristic waveforms of 0.25 s length for three of the channels along the east-west line are shown. Note the decreasing amplitude and sharpness of the shocks. The peak frequency is in the range of 11-15 Hz, slightly into the infrasound regime.

4. LAUNCH TRACKING ANALYSIS

There were two stations that were set up as 5-m diameter intensity probes.[18] Figure 5 shows the layout of one of these probes. In both cases the line from the center microphone toward microphone 2 pointed at the launch pad. One probe was located at a distance of 330 m from the pad and the other was on a mountaintop location approximately 6 km from the pad and about 500 m above the level of the launch pad.

To track the launch vehicle, the dataset is first divided into 1/2 second blocks. The signals for all four channels in each block are cross-correlated with each other to find the delay of each channel relative to the other three channels. These delays are the input data to a least-squares fit to a plane-wave model of the sound source. The output parameters of the fit are the two angles characterizing the direction to the sound source, the azimuthal angle, ϕ , relative to the microphone 1-to-2 line, and the inclination angle above the

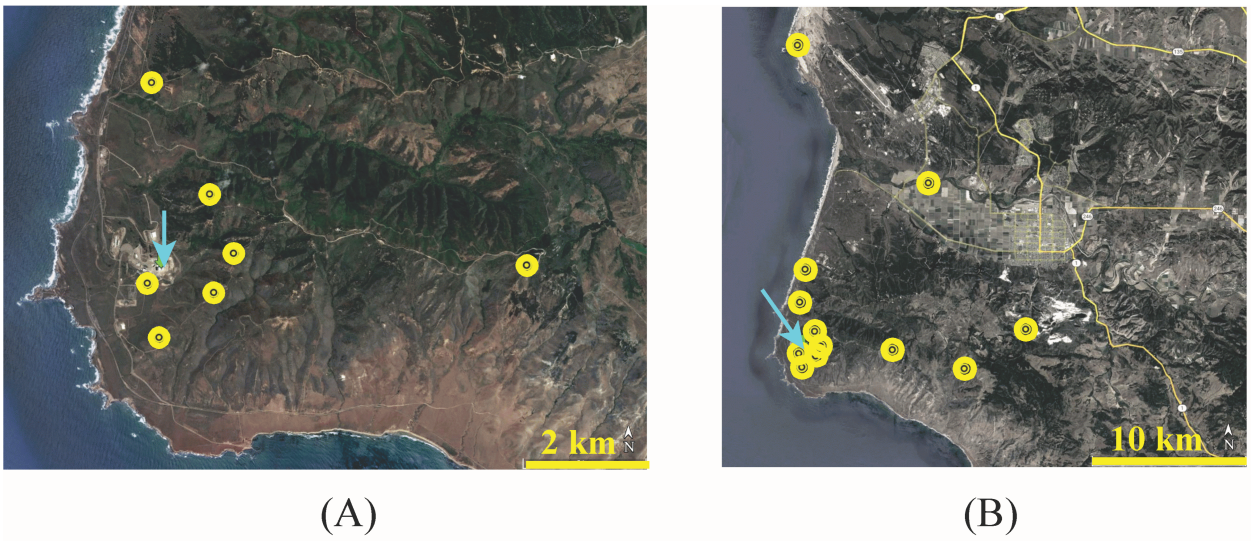

Figure 2: Google Earth images showing the positions of the recording stations. The position of the launch pad is shown by the blue arrow. The measuring stations are shown by the yellow target icons. The figures are oriented so that the top of the figure is north. Part (A) shows those stations that are close to the pad, while part (B) shows all the stations. The close stations form an arc around the east side of the launch pad, while the more distant stations form a roughly east-west radial and a roughly north-south radial. Map data: Google, CSUMB SFML, CA OPC, image ©2022 Maxar Technologies

horizon, θ. We assume that the rocket travels in a well-defined plane, which is generally true during the first few minutes of a launch. The intersection of the direction to the source with that launch plane determines the inferred position of the sound source.

It is difficult to determine a sound source inclination when the angle is near zero. The arrival time of a signal at an outer microphone relative to the center microphone depends on $\cos(\theta)$, where θ is the angle of inclination, and the sensitivity of the cosine function to changes in θ at $\theta = 0$ is very small. The inclination angle is not determined accurately until $\theta \approx 10°$. It is also difficult to determine the azimuthal angle when $\theta \approx 90°$ because the wave is then coming almost straight down onto the probe, and the signals arrive at all the channels nearly simultaneously.

We are able to compare our inferred positions with the rocket's actual position because we used a GPS clock signal to get absolute timing of all of these channels, and we received telemetry and timing data of the actual trajectory from Vandenberg Space Force Base after the launch. Knowing the launch plane and source direction we can determine the distance, and therefore the propagation delay of the sound, allowing us to compute when the sound was emitted from the source. The speed of sound was assumed to be 340 m/s (consistent with the temperature at the launch pad) for low altitudes. When the rocket was at significantly higher altitudes we assumed an average speed of 335 m/s, consistent with the colder temperatures at those altitudes.

A. NEAR PAD LOCATION

Figure 6 shows the geometry of the intensity probe near the launch pad (330 m away.) The red line on the plot shows the direction of the flame trench under the rocket. The blue line shows the plane of the rocket's trajectory. The yellow line shows the orientation of the probe toward the launch pad, and the green line shows the direction that intersects the flame trench about 80 m away from the rocket. This line represents the measured direction of the apparent maximum source of sound before the rocket lifts off from the pad.

Figure 7 shows the results of this analysis on this close data. The engines are ignited several seconds

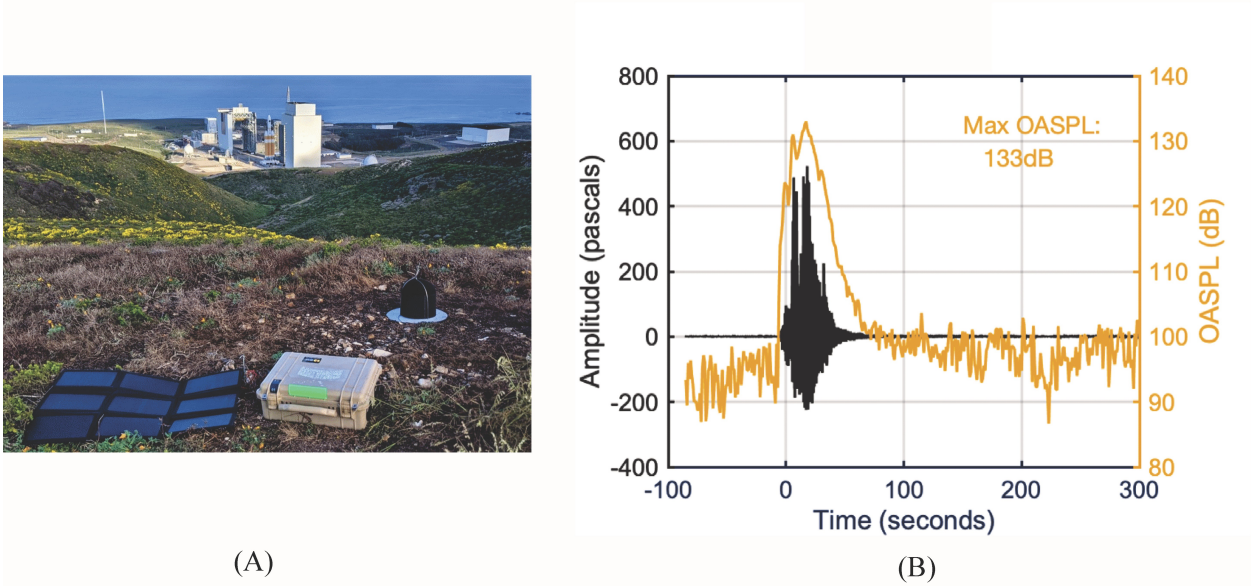

Figure 3: ***Part (A) shows the position of one measuring station relative to the pad. Part (B) shows both the amplitude of the pressure signal measured at this station (black, on the left axis) and the OASPL of the signal (gold, on the right axis.) Note the asymmetry of the pressure waveform; the positive excursions are much larger than the negative. Also, because of wind noise there is a noise floor of 92-97 dB at this location. This station is located 960 m from the launch pad.***

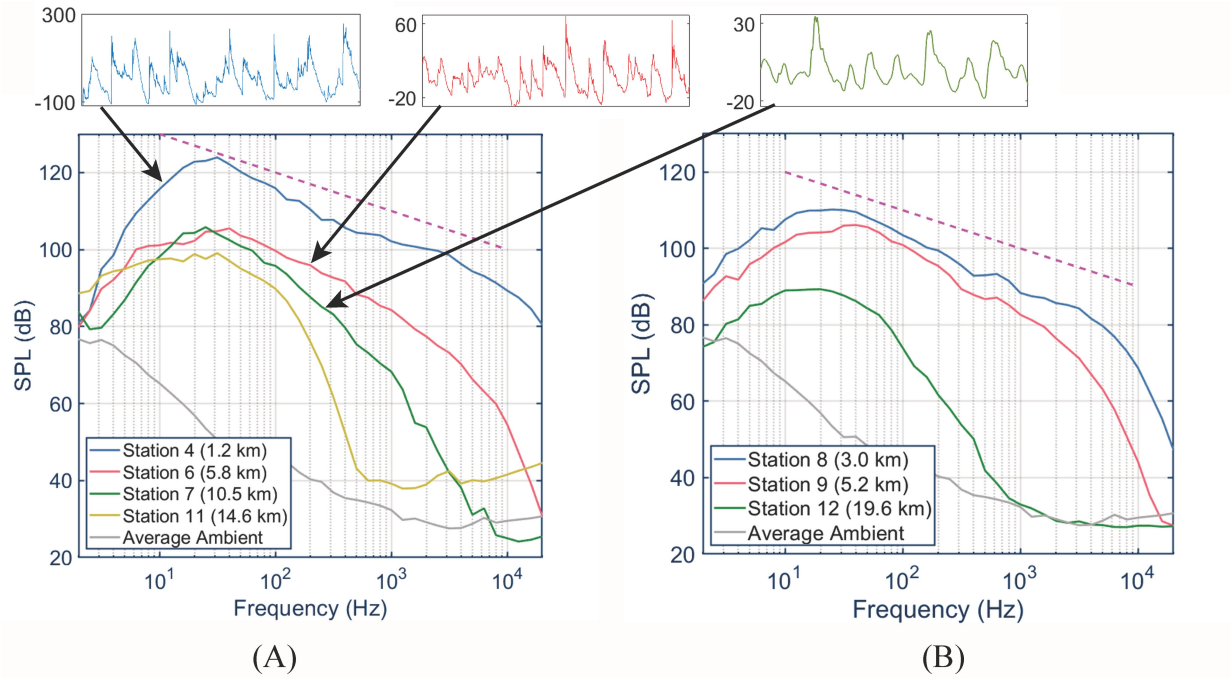

Figure 4: ***Part (A) shows how the spectrum varies along an east-west line from the launch pad. Part (B) shows the variation along a north-south line. Note the dashed line with a slope of 10 dB/decade for comparison with the data. Note the earlier roll-off of the higher frequencies from 10 dB/decade as the propagation distance increases. The closer stations show spectral evidence of significant shocks in the signal. Typical waveforms for three of the stations along the east-west line are shown. The y-axis on these insets is measured in Pa, the x-axis is time. Each inset shows 0.25 seconds. Note the decreasing strength and sharpness of the shocks. At all stations the peak frequency is in the 11-15 Hz range.***

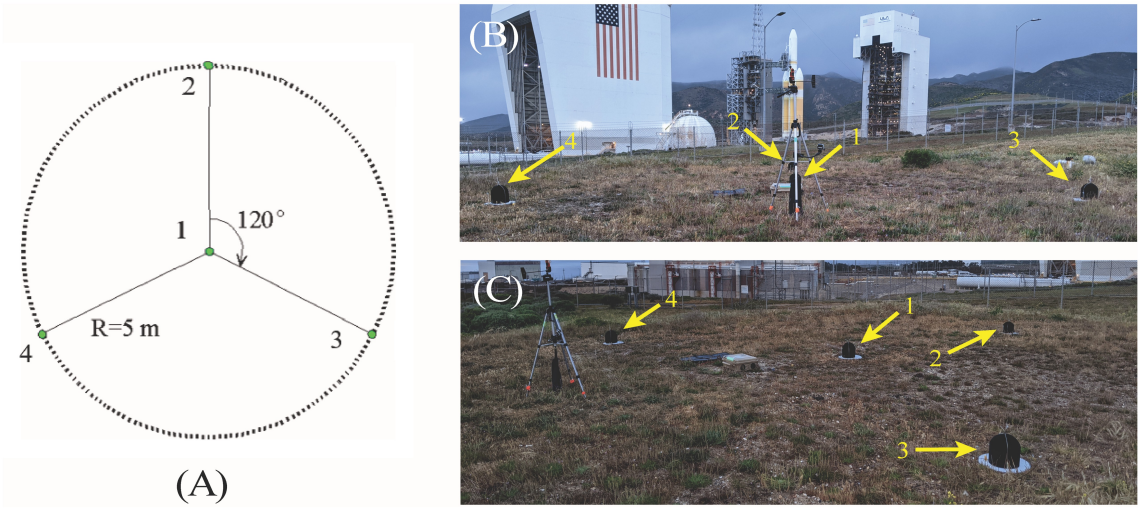

Figure 5: The layout of an intensity probe. Part (A) shows the spacing of the microphones. The radius of the circle is 5 meters, and the outer microphones are spaced apart by 120°. The line from microphone 1 to microphone 2 pointed at the launch pad in both cases. Part (B) is a photograph of the near intensity probe with the microphones (inside their windscreens) identified with the numbers 1-4. The probe is pointed toward the launch pad. Part (C) shows the same probe from a different angle.

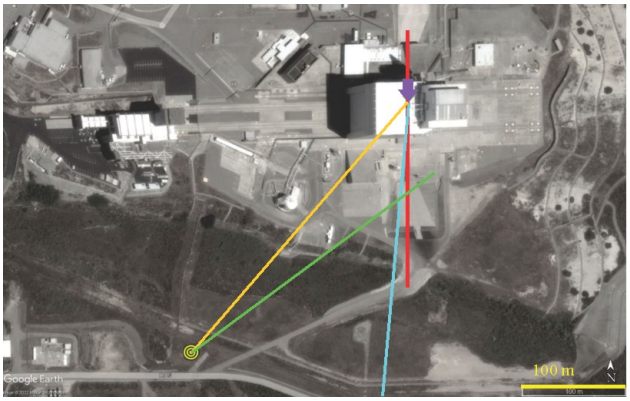

Figure 6: The geometry of the tracking measurement for the close intensity probe. The yellow target indicates the measurement location, and the violet arrow shows the location of the launch pad (under the assembly building) The red line shows the direction of the flame trench. The plume exits along the ground along this line before the rocket lifts off. The blue line indicates the plane of the rocket's trajectory when launched. The yellow line shows the orientation of the intensity probe, and the green line indicates the measured direction of the sound source before take-off, while the jet comes out of the flame trench. Map data: Google, CSUMB SFML, CA OPC, image ©2022 Maxar Technologies

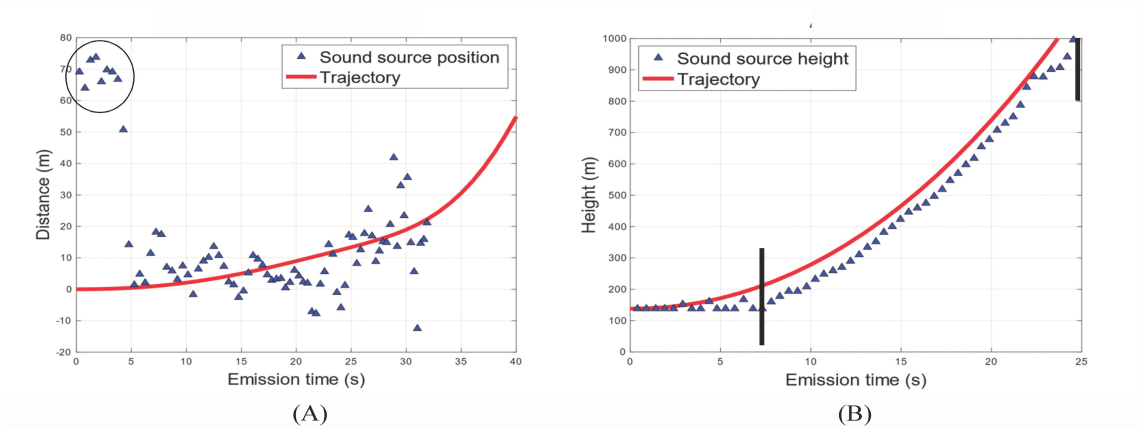

Figure 7: The position of the noise source from the rocket plume as a function of time. Part (A) shows the downrange distance. Before $T = 5$ seconds the noise is coming from the flame trench, as indicated by the oval on the figure. After the source emerges from the flame trench the sound tracks the rocket's position, as shown by the trajectory curve. Part (B) shows the inferred height of the source. The source doesn't emerge above the launch pad until about $T = 8$ seconds. Note that the source position is always below the rocket, as shown by the trajectory information. The average distance below the nozzles of the engine during the time between the two vertical bars on the graph is 55 m. The trajectory curves are from telemetry data from Vandenberg Space Force Base. The time of the acoustic data is corrected for the acoustic propagation delay from the rocket.

before the rocket is released in order to get full thrust before release. While the rocket is held down, the plumes from the engines come out of the flame trenches on both sides of the launch pad. The red line in Fig. 6 shows the direction of the plume coming out of the flame trench. In the figures $T = 0$ represents the time of release of the rocket. It takes about 8 seconds after release before the sound source region of the plume emerges from the flame trench and the the intensity probe has a direct line to it.

As can be seen in Fig. 7(A), between $T = 0$ and about $T = 5$ the sound source is about 60-80 m away from the launch pad. This corresponds to the green line in Fig. 6, where the sound is originating from the flame trench. At about $T = 5$, as the rocket rises, the plume moves back toward the pad and eventually the sound source emerges from the surface of the pad at a downrange distance of 0 m. As this plot shows, during the first 30 seconds the rocket doesn't travel far downrange; it is mostly going straight upward, but the average of the downrange data follows the trajectory well. The red line showing the rocket's actual trajectory is from telemetry received from Vandenberg Space Force Base. The time of the points on the plot are adjusted for the acoustic propagation delay from the rocket to the receiving station. We used a sound speed of 340 m/s, consistent with the temperature at the launch pad at the time of launch.

Figure 7(B) shows the height inferred from the tracking direction and the launch plane. The altitude shown is height above sea level and includes the 130 m altitude of the launch pad. Note that it takes about 8 seconds for the sound source to rise above the launch pad height. It is notable that the source altitude is always below the rocket altitude, which is the position of the nozzles of the engine. If we average the distance of the source below the rocket nozzles during the time between the two vertical bars on the graph, we find that it is located about 55 m below the rocket. This position is noted in the picture of the rocket shown in Fig. 1. Previous work has shown that the sound source should be about 17 nozzle diameters below the nozzle exit.[1] The measured distance of 55 m is intermediate between 17 single nozzle diameters (41 m) and 17 times the effective diameter of three nozzles combined (71 m). This implies that the sound source is from a part of the plume where where the plumes no longer behave individually (which would correspond to

Figure 8: A Google Earth plot showing the location of the mountaintop intensity probe relative to the launch pad. The green arrow shows the launch pad location. The yellow lines show the orientation of both intensity probes. Map data: Google, CSUMB SFML, CA OPC, image ©2022 Maxar Technologies

the 41 m distance), but do not yet totally behave as a fully merged, single plume (which would correspond to a distance of 71 m.) This seems to correspond to what can be seen visually in Fig. 1. The position tracking becomes unreliable after about 25 or 30 seconds for this station because the noise is coming from almost straight overhead and we lose almost all directional sensitivity. By the time it has moved sufficiently downrange to regain directionality, the signal is lost in the substantial wind noise that was present during the measurement.

B. MOUNTAINTOP LOCATION

Figure 8 shows the location of the second intensity probe relative to the launch pad. It was about 6 km away at an altitude of about 500 m above the launch pad. The intensity probe was located on a parking lot, and it did not have a direct line to the rocket until the rocket rose above the elevation of the parking lot. Figure 9 shows the altitude and downrange data from this probe.

The altitude measurement is not reliable until the angle reaches about 8° above the horizontal, because of the insensitivity of the cosine function at small angles. The downrange measurement has relatively large uncertainties because of the 6-km long distance from the source making small angular errors into larger distance errors, and possibly propagation effects, such as winds and temperature fluctuations aloft. We used a sound speed of 335 m/s as an average propagation speed, given the lower temperatures at higher altitudes. We do not recompute the source offset for this data because that offset corresponds to an angle of less than 0.5° at a distance of 6 km, which is less than the angular uncertainty in the data.

With more than one intensity probe it is possible to track the position of the rocket without prior knowledge of the trajectory plane. Unfortunately, that cannot be done in this case because the close intensity probe loses position sensitivity at about the same time that the distant probe gains position sensitivity, at about 25-30 seconds after launch.

5. OASPL, PEAK DIRECTIVITY, AND SOUND POWER LEVEL

Using the trajectory information from Vandenberg Space Force Base and our measurements at multiple locations, we are able to determine the maximum OASPL of the rocket and the directivity of the launch noise relative to the rocket's plume. If a measuring station is located at a position (x, y, z) relative to the launch pad, with x pointing east, and the rocket is located at (x', y', z') at a given time and the plume is

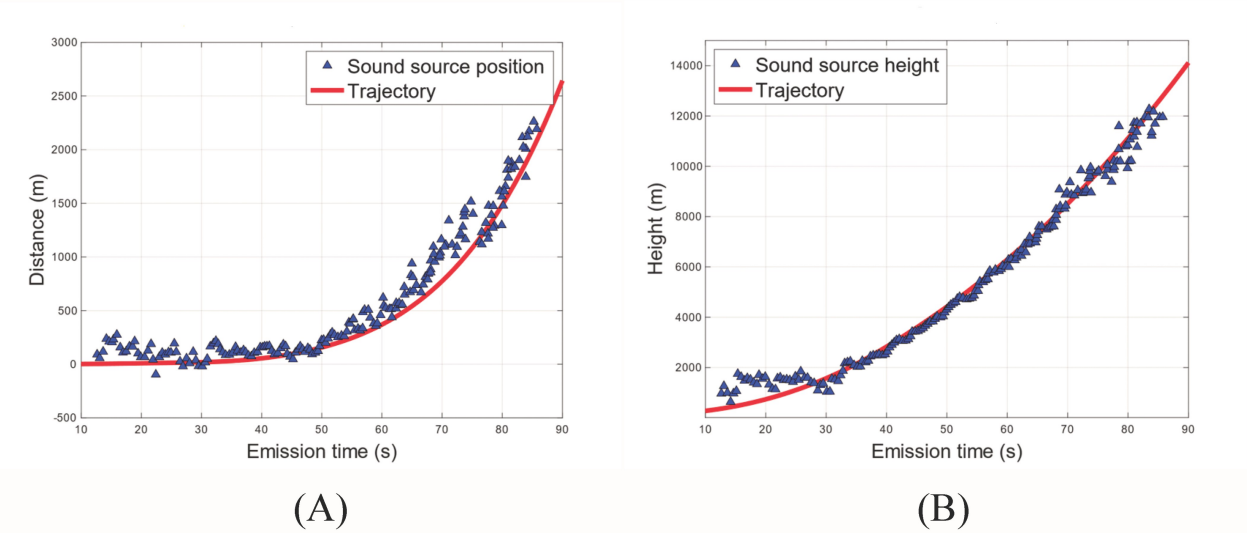

Figure 9: Part (A) shows the downrange distance as measured from the mountaintop location, compared to the known trajectory information. Part (B) shows the altitude of the rocket compared to the trajectory.

assumed to be pointing directly backward along the trajectory, the angle of the measuring station relative to the plume can be calculated from

$$\cos(\theta) = \frac{[\sin(\alpha)(\sin(\phi)(x - x') + \cos(\phi)(y - y')) - \cos(\alpha)(z - z')]}{r}, \tag{1}$$

where r is the distance from rocket to station, α is the angle the trajectory makes with the vertical, and ϕ is the azimuthal angle between the current trajectory and the y axis.

As an example of how this can be used, in Fig. 10 we show the OASPL vs. time for the mountaintop station, corrected for spherical spreading to a distance of 100 effective nozzle diameters (420 m) from the rocket (blue line). It also shows the angle relative to the plume as a function of time, calculated from the above equation and delayed to account for sound propagation at 340 m/s to the station (black line). We can find the peak directivity angle and maximum OASPL by fitting a cubic curve to the OASPL vs. angle. From the fit coefficients we can find the maximum OASPL and corresponding angle. We use a cubic fit because OASPL vs. angle is not symmetric about the peak and a quadratic fit is always symmetric. We do the fit over the angular range from $45°$ to $85°$, because this is centered where we expect the peak directivity to be. The magenta line in the figure shows the fit for this station transformed to be plotted versus time. The asterisks mark the position of the peak OASPL and corresponding angle.

If we do this fit over different angular ranges ($45° - 90°$ or $50° - 85°$, for example) we can get an idea of the variability of these fit results. The mean and standard deviation of the set of fits done over different angular ranges are the value and uncertainty of the peak directivity for a given station. Using that information we get the results shown in Table 1. Using a weighted average where the weight of a point is the reciprocal the uncertainty and the data given in the table, we get a peak directivity angle of $70.4 \pm 2.1°$.

Because the far-field directivity is controlled by Mach-wave radiation from the supersonic exhaust plume, we expect the peak directivity to correspond to an angle of

$$\theta_p = \cos^{-1}\left(\frac{1}{M_c}\right), \tag{2}$$

where M_c is the Oertel Mach number, given by

$$M_c = \frac{U_j + 0.5c_j}{c_j + c_a} \tag{3}$$

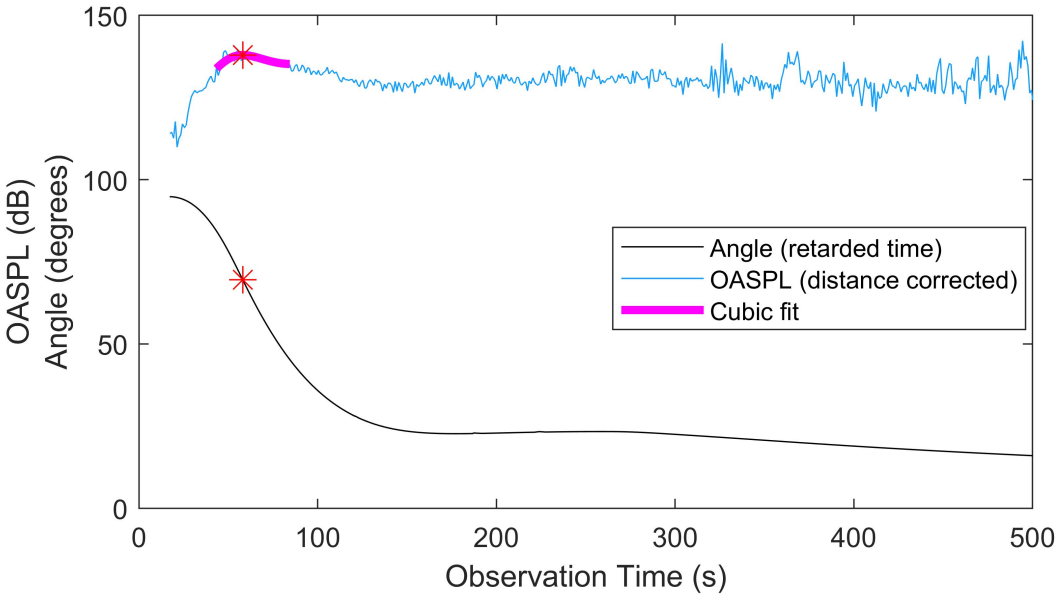

***Figure 10:** The blue curve shows OASPL vs. time, corrected for spherical spreading to a distance of 100 effective nozzle diameters (420 m). This is for the mountaintop location. The black curve is the angle of the station relative to the rocket plume for the sound being detected at that time. The magenta curve is a cubic fit of OASPL vs. angle (transformed to OASPL vs. time). The red asterisks show the max OASPL and corresponding angle derived from the fit.*

***Table 1:** Peak directivity derived from each station. Station 5 acquired no data because of interference from a nearby radar station. Station 11 was shielded by terrain during the relevant part of the rocket's ascent.*

Station	**Distance** (km)	**Peak directivity** (degrees)	**Uncertainty** (degrees)	**Station**	**Distance** (km)	**Peak directivity** (degrees)	**Uncertainty** (degrees)
1	0.330	70.2	0.8	7	10.5	67.5	1.7
2	1.12	74.0	0.6	8	3.07	69.4	0.8
3	0.96	71.0	0.6	9	5.29	69.3	2.0
4	1.23	62.8	4.6	10	13.5	69.4	1.1
6	5.84	69.5	0.8	12	19.7	70.4	0.8
			Weighted mean	70.4	$\pm$ 2.1		

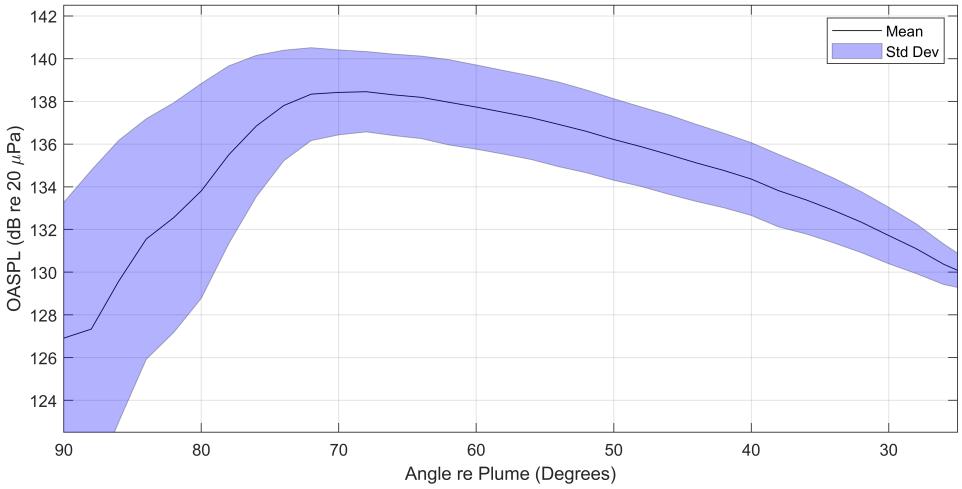

Figure 11: OASPL vs. angle, averaged over all the stations. The shaded area shows the standard deviation of the measurement. Note that this curve is consistent with a peak directivity angle of about $70°$**.**

where c_j is the speed of sound at the exit of the jet, c_a is the speed of sound in the ambient air, and U_j is the fully expanded jet velocity.[19–22] Using estimated parameters[23] of the RS-68A engines, $U_j \approx 3750$ m/s and $c_j \approx 1100$ m/s, we calculate a predicted peak directivity of $70°$, in good agreement with the measured value of $70.4°$.

Figure 11 shows the angular dependence of the OASPL averaged over the stations. We can integrate the sound power over all inclination angles, using the fact that there is almost no power radiated in the forward hemisphere,[24] and as can be seen by the $\sim$10 dB drop in the OASPL as we approach $90°$, and assuming axisymmetry. Doing so, we get a total sound power level of 197 dB. When we compare this with the total mechanical power of the Delta IV Heavy rocket of 16.5 GW, we find that this rocket has a sound production efficiency of 0.3%, somewhat lower than the 0.5% frequently used to estimate sound power,[25] but in line with some other recent measurements.[26] We note that the impact of a finite-impedance ground on sound power estimates is not well understood and should be the subject of future work.

6. CONCLUSION

We were able to measure a number of different characteristics of the Delta IV Heavy launch on April 26, 2021. When the rocket was first ignited, the sound mainly came from the flame trench. As the rocket lifted off, the apparent maximum sound source was about 55 m below the nozzle of the rocket engines. We were able to accurately track the rocket's position using multimicrophone probes and a knowledge of the launch plane. The peak directivity angle of the sound is at $70 \pm 2°$ and the total sound power level is 197 dB. This corresponds to a sound power efficiency of about 0.3%, somewhat lower than what is usually assumed.

ACKNOWLEDGMENTS

We appreciate the cooperation of Vandenberg Space Force Base for allowing us access to make these measurements.

REFERENCES

[1] C. P. Lubert, K. L. Gee, and S. Tsutsumi, "Supersonic jet noise from launch vehicles: 50 years since NASA SP-8072." J. Acoust. Soc. Am., **151**, 752-791 (2022).

[2] J. N. Cole, H. E. Von Gierke, D. T. Kyrazis, K. M. Eldred, and A. J. Humphrey, "Noise radiation from fourteen types of rockets in the 1,000 to 130,000 pounds thrust range", WADC Technical Report No. 57, 354 (1957).

[3] W. H. Mayes, W. E. Lanford, and H. H. Hubbard, "Near-field and far-field noise surveys of solid-fuel rocket engines for a range of nozzle exit pressures," NASA Report No. TN D-21 (Langley Research Center, National Aeronautics and Space Administration, Hampton, VA, 1959).

[4] W. H. Maynes and P. M. Edge, "Noise measurements during captive and launch firings of a large rocket-powered vehicle," NASA TN D-1502 (Langley Research Center, National Aeronautics and Space Administration, Hampton, VA, 1962).

[5] S. H. Guest, "Acoustic efficiency trends for high thrust boosters," NASA TN D-1999 (George C. Marshall Space Flight Center, National Aeronautics and Space Administration, Huntsville, AL, 1964).

[6] R. N. Tedrick, "Acoustical measurements of static tests of clustered and single-nozzled rocket engines," J. Acoust. Soc. Am. **36**, 2027–2032 (1964).

[7] R. C. Potter and M. J. Crocker, "Acoustic prediction methods for rocket engines, including the effects of clustered engines and deflected exhaust flow," NASA-CR-566 (George C. Marshall Space Flight Center, National Aeronautics and Space Administration, Huntsville, AL, 1966).

[8] S. A. McInerny, "Launch vehicle acoustics. 1—Overall levels and spectral characteristics," J. Aircr. **33**, 511–517 (1996).

[9] S. A. McInerny, "Launch vehicle acoustics. 2—Statistics of the time domain data," J. Aircr. **33**, 518–523 (1996).

[10] S. A. McInerny, J. K. Wickiser, and R. H. Mellen, "Rocket Noise Propagation," ASME Noise Control Acoust. **24**, 37–50 (1997).

[11] S. A. McInerny, G. Lu, and S. Ölçmen, "Rocket and Jet Mixing Noise, Background and Prediction Procedures," National Center for Physical Acoustics Report No. UM 03-08-013 (National Center for Physical Acoustics, University, MS, 2004).

[12] S. A. McInerny, "Characteristics and predictions of far-field rocket noise," Noise Control Eng. J. **38**, 5–16 (1992).

[13] S. A. McInerny and S. M. Ölçmen, " High-intensity rocket noise: Nonlinear propagation, atmospheric absorption, and characterization," J. Acoust. Soc. Am. **117**, 578–591 (2005).

[14] K. L. Gee, D. J. Novakovich, L. T. Mathews, M. C. Anderson, and R. D. Rasband. "Development of a Weather-Robust Ground-Based System for Sonic Boom Measurements." NASA/CR-2020-s5501870 (2020).

[15] M. C. Anderson, K. L. Gee, D. J. Novakovich, L. T. Mathews, and Z. T. Jones, 2020, December. "Comparing two weather-robust microphone configurations for outdoor measurements." Proc. Mtgs. Acoust. **42**, 040005. (2020).

[16] K. L. Gee, T. B. Neilsen, A. T. Wall, J. M. Downing, M. M. James, and R. L. McKinley, "Propagation of crackle-containing noise from military jet aircraft," Noise Control Eng. J. 64, 1-12 (2016).

[17] S. N. Gurbatov and O. V. Rudenko, "Statistical Phenomena," in Nonlinear Acoustics, edited by M. F. Hamilton, and D. T. Blackstock, Academic Press, San Diego, CA, pp. 377–398. This reference discusses 20 dB/decade for a narrowband spectrum. Our 10 dB/decade roll-off results from integration to the one-third-octave spectrum.

[18] F. J. Irarrazabal, M. R. Cook, K. L. Gee, T. P. Nelson, D. J. Novakovich, and S. D. Sommerfeldt, "Initial infrasound source characterization using the phase and amplitude gradient estimator method." Proc. Mtgs. Acoust. **36**, 045004 (2019).

[19] B. Greska, A. Krothapalli, W. C. Horne, and N. Burnside, "A Near-Field Study of High Temperature Supersonic Jets," in Proceedings of the 14th AIAA/CEAS Aeroacoustics Conference (29th AIAA Aeroacoustics Conference), Vancouver, BC (May 5–7, 2008), AIAA 2008-3026.

[20] L. C. Sutherland, "Progress and problems in rocket noise prediction for ground facilities," in Proceedings of the 15th AIAA Aeroacoustics Conference, Miami, FL (May 11–13, 1993), AIAA-93-4383.

[21] C. K. W. Tam, "Mach wave radiation from high-speed jets," in Proceedings of the 47th AIAA Aerospace Sciences Meeting, Orlando, FL (January 5–8, 2009), AIAA 2009-13.

[22] J. M. Seiner, M. K. Ponton, B. J. Jansen, and N. T. Lagen, "The Effects of Temperature on Supersonic Jet Noise Emission," in DLGR/AIAA 14th Aeroacoustics Conference, Vancouver, BC (May 5–7, 1992), DLGR/AIAA 92-02-046.

[23] Paramters estimated using the NASA-Glenn Chemical Equilibrium Program CEA2. NASA Glenn Research Center, "Chemical equilibrium with applications CEARUN," https://cearun.grc.nasa.gov/ (Last date accessed: 25 Oct 2021).

[24] Kenny, R. J., Hobbs, C, Plotkin, K, Pilkey, D, "Measurement and Characterization of Space Shuttle Solid Rocket Motor Plume Acoustics," 15th AIAA/CEAS Aeroacoustics Conference (30th AIAA Aeroacoustics Conference). 2009.

[25] K. M. Eldred, "Acoustic loads generated by the propulsion system," NASA SP-8072 (National Aeronautics and Space Administration, Washington, DC, 1971).

[26] L. T. Mathews, K. L. Gee, and G. W. Hart (2021). Characterization of Falcon 9 launch vehicle noise from far-field measurements. J. Acoust. Soc. Am. **150**, 620-633 (2021)